Mixing strength in the two lowest 0^- states in ^{208}Pb

A. Heusler*
Max-Planck-Institut für Kernphysik, D-69029 Heidelberg, Germany

G. Graw, R. Hertenberger, and F. Riess
Department für Physik, Ludwig-Maximilian-Universität München, D-85748 Garching, Germany

H.-F. Wirth
Physik Department E18, Technische Universität München, D-85748 Garching, Germany

R. Krücken
Physik Department E12, Technische Universität München, D-85748 Garching, Germany

P. von Brentano
Institut für Kernphysik, Universität zu Köln, D-50937 Köln, Germany
(Received 16 November 2006; published 28 February 2007)

With a resolution of 3 keV, the two lowest 0^- states in ^{208}Pb are identified by measurements of the reaction ^{207}Pb(d, p) with the München Q3D magnetic spectrograph in the region $E_x = 5.2$–5.7 MeV where the average level spacing is 6 keV. Precise relative spectroscopic factors are determined. Matrix elements of the residual interaction among one-particle one-hole configurations in a two-level scheme are derived for the two lowest 0^- states in ^{208}Pb. The off-diagonal mixing strength is determined as 110 ± 10 *(experimental)* $\pm$ 15 *(systematic)* keV. Measurements of the reaction ^{208}Pb(p, p') via isobaric analog resonances in ^{209}Bi support the structure information obtained.

DOI: 10.1103/PhysRevC.75.024312 PACS number(s): 21.10.Jx, 21.10.Hw, 25.45.Hi, 27.80.+w

I. INTRODUCTION

The nucleus ^{208}Pb offers the singular chance to study a two-level scheme in the space of shell model configurations. Below $E_x = 6.1$ MeV, only two 0^- states among about 120 one-particle one-hole configurations are expected from shell model calculations [1,2]. They have been identified [3], but their structure is not known in detail. With the average residual interaction known from experiment [4,5], they are predicted to consist essentially of the two lowest configurations $s_{1/2}p_{1/2}$ and $d_{5/2}f_{5/2}$, since the next particle-hole configuration is ten times more distant than a mean matrix element (m.e.) of the residual interaction among one-particle one-hole configurations.

We took spectra of the reaction ^{207}Pb(d, p) at a resolution of 3 keV [6] up to $E_x = 8$ MeV and identified the two 0^- states in the region $E_x = 5.2$–5.7 MeV, where the mean level distance is 6 keV.

Most of the low-lying states in ^{208}Pb are considered as excited states created by the coupling of exactly one particle and one hole to the ground state. We postulate that each particle-hole state is completely described as a mixture of a few particle-hole configurations. The ground state of ^{207}Pb is assumed to be a pure $p_{1/2}$ neutron-hole state in relation to the ground state of ^{208}Pb. In the ^{207}Pb(d, p) reaction, the particle-hole states in ^{208}Pb with spin 0^- are populated by $L = 0$ transfer only, whereas the 1^- states are populated by both $L = 0$ and $L = 2$ transfer.

For two spin 0^- and nine 1^- states below $E_x = 6.5$ MeV, relative spectroscopic factors are measured. Using the method of Ref. [4] and assuming the two lowest configurations to be almost completely contained in the two lowest 0^- states, we deduced matrix elements of the residual interaction between the 0^- configurations $s_{1/2}p_{1/2}$ and $d_{5/2}f_{5/2}$.

Results of the inelastic proton scattering on ^{208}Pb via isobaric analog resonances (IAR) in ^{209}Bi populating the two 0^- states and some 1^- states [6,7] are discussed.

II. RESIDUAL INTERACTION IN THE SHELL MODEL

A. Determination of matrix elements of the residual interaction

We consider states with a certain spin I and a certain parity π. In order to distinguish states from configurations, we use the notation $|n, I^\pi\rangle$ for configurations and $\underline{|n, I^\pi\rangle}$ for states. Because of the dense spacing of states, some doublets are not yet resolved, and some spins and parities are not yet known. Therefore, often the alternative notation $\underline{|E_x, I^\pi\rangle}$ (simplified to 5280 0^-, e.g.) for states is used, as was done in Ref. [6].

In the shell model, the states are described to consist of particle-hole configurations $|k, I^\pi\rangle$,

$$\underline{|n, I^\pi\rangle} = \sum_k t_{nk}(I^\pi)|k, I^\pi\rangle. \quad (1)$$

*Corresponding author. Email address: A.Heusler@mpi-hd.mpg.de

Inversely, the particle-hole configurations can be described by the physical states as

$$|k, I^\pi\rangle = \sum_n t^\dagger_{nk}(I^\pi)|\underline{n, I^\pi}\rangle. \quad (2)$$

Here $t_{nk}(I^\pi)$ denotes the unitary transformation matrix of the Hilbert space of the physical states $|\underline{n, I^\pi}\rangle$ into the configuration space $|k, I^\pi\rangle$. It is real because of the time reversal invariance of the Hamiltonian. The Hamiltonian $\mathbf{H}$ acting on the states $|\underline{n(I)}\rangle$ has the eigenvalues $E_n(I^\pi)$,

$$H_{nm}(I^\pi) = \delta_{nm} E_n(I^\pi), \quad (3)$$

and the Hamiltonian $\mathbf{h^0}$ acting on the configurations $|k, I^\pi\rangle$ has the eigenvalues $e^0_k(I^\pi)$,

$$h^0_{kl}(I^\pi) = \delta_{kl} e^0_k(I^\pi). \quad (4)$$

They differ by the residual interaction

$$v_{kl}(I^\pi) = \langle k(I^\pi)|\mathbf{H} - \mathbf{h^0})|l, I^\pi\rangle \quad (5)$$

or explicitly

$$v_{kl}(I^\pi) = \sum_{nm} t_{kn}(I^\pi) H_{nm}(I^\pi) t^\dagger_{ml}(I^\pi) - h^0_{kl}(I^\pi). \quad (6)$$

B. Truncated configuration space

From experiments, amplitudes $\mathbf{t}$ for a *subset* of states can be derived only. When a lower part of the configuration space is separated from the higher configurations by a gap Δ sufficiently large in relation to an average m.e., the m.e. of the residual interaction can be determined in the truncated configuration space by the method described in Ref. [4].

Among all levels adopted by the Evaluated Nuclear Structure Data File [8,9] in doubly magic nuclei (including ^{88}Sr and ^{90}Zr), few 0^- states are known. In ^{4}He, three 0^- states are known; in ^{16}O, two 0^- states with different isospin and in ^{40}Ca, two 0^- states are known. Only in ^{208}Pb are bound 0^- states known. So, the 0^- doublet represents a unique case of two-level mixing, especially in view of the extremely large distance Δ to the next 0^- configuration according to shell model calculations, see Fig. 1.

The lowest negative parity states in ^{208}Pb are assumed to be well described by the shell model as particle-hole states in relation to the ground state of ^{208}Pb. Especially, the two lowest 0^- states, $|\underline{1(0^-)}\rangle$ and $|\underline{2(0^-)}\rangle$ at $E_x = 5280$ and 5599 keV, respectively, are assumed to consist of the neutron particle-hole configurations $|s_{1/2}p_{1/2}, 0^-\rangle$ and $|d_{5/2}f_{5/2}, 0^-\rangle$ with weak admixtures of higher configurations $|C_q, 0^-\rangle$,

$$\begin{aligned}|\underline{1, 0^-}\rangle &= t_{11}(0^-)|s_{1/2}p_{1/2}, 0^-\rangle + t_{12}(0^-)|d_{5/2}f_{5/2}, 0^-\rangle \\ &\quad + \sum_{q>2} t_{1q}(0^-)\,|C_q, 0^-\rangle, \\ |\underline{2(0^-)}\rangle &= t_{21}(0^-)|s_{1/2}p_{1/2}, 0^-\rangle + t_{22}(0^-)\,|d_{5/2}f_{5/2}, 0^-\rangle \\ &\quad + \sum_{q>2} t_{2q}(0^-)\,|C_q, 0^-\rangle. \end{aligned} \quad (7)$$

In the following, amplitudes $\mathbf{t}$ are derived from experimental data, and the m.e. of the residual interaction can be determined in the truncated configuration space as

$$\begin{aligned} v_{kl}(I^\pi) &= \sum_{n=1,2} t_{kn}(I^\pi) t_{ln}(I^\pi) \\ &\quad \times \left[E_n(I^\pi) - \frac{1}{2}\left(e^0_k(I^\pi) + e^0_l(I^\pi)\right)\right] + r_{kl}(I^\pi). \end{aligned} \quad (8)$$

As extensively explained in Ref. [4], the residual matrix $r_{kl}(I^\pi)$ describes the influence of the higher configurations in the space separated from the lower configurations by the gap Δ. In our application, the residual matrix $\mathbf{r}$ is negligible.

In the truncated configuration space, the unitarity relation of matrix $\mathbf{t}$ is only approximately valid, that is,

$$\sum_{n=1,2} t_{kn}(I^\pi) t^\dagger_{ln}(I^\pi) = \delta_{kl} - d_{kl}(I^\pi) \approx \delta_{kl}. \quad (9)$$

The deviation matrix $d_{kl}(I^\pi)$ is introduced to derive an estimate of the systematic uncertainty of the m.e. of the residual interaction.

C. Two-level scheme of the lowest 0^- states

The two-level scheme is valid if the amplitudes $t_{1q}(0^-)$ and $t_{2q}(0^-)$ are small, thus allowing us to truncate the configuration space to two configurations. We postulate the deviation from unitarity to be small in the truncated two-level space,

$$\begin{vmatrix} d_{11}(0^-)\; d_{12}(0^-) \\ d_{21}(0^-)\; d_{22}(0^-) \end{vmatrix} \approx \begin{pmatrix} 0\;0 \\ 0\;0 \end{pmatrix}. \quad (10)$$

By adding a fictitious third configuration with energy $e^0_3(0^-) \approx e^0_2(0^-) + \Delta$ (see Fig. 1) from upper limits of the deviation matrix $|\mathbf{d}|$, the value $\mathbf{r}$ as an estimate for the systematic error of the residual interaction $\mathbf{v}$ is determined. Indeed, the systematic error is estimated to be similar to the experimental error.

D. Determination of amplitudes by ^{207}Pb(d, p)

The ground state of ^{207}Pb is a rather pure single-neutron-hole state with the configuration $|p_{1/2} \otimes {}^{208}\text{Pb, g.s.}\rangle$. Hence, in 0^- states of ^{208}Pb, the ^{207}Pb(d, p) reaction populates the $s_{1/2}p_{1/2}$ component only. This allows us to determine the amplitudes $t_{11}(0^-)$ and $t_{21}(0^-)$ in Eq. (7).

In contrast, for spin 1^-, two configurations, $s_{1/2}p_{1/2}$ and $d_{3/2}p_{1/2}$, are excited by the ^{207}Pb(d, p) reaction. According to shell model calculations, $d_{3/2}p_{1/2}$ is the fifth configuration. Up to $E_x = 6.5$ MeV, nine 1^- states are identified as expected from the shell model (see later in Table III). Each of them can

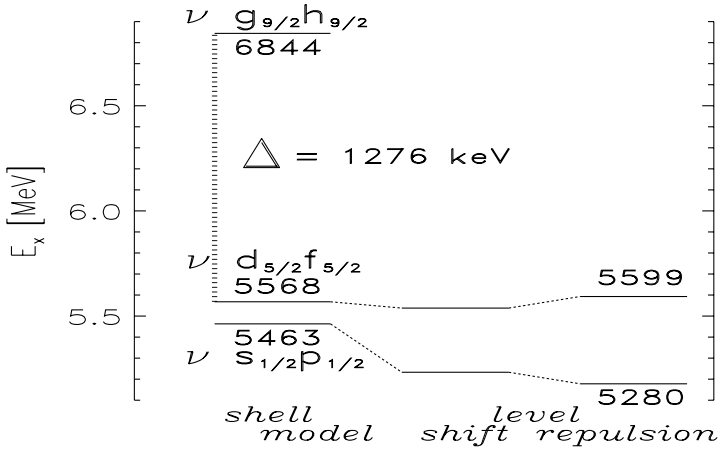

FIG. 1. Two lowest 0^- configurations in ^{208}Pb, neutron particle-hole configurations $s_{1/2}p_{1/2}$ and $d_{5/2}f_{5/2}$, are separated from the next higher configurations by a large gap Δ, allowing us to discuss the simple case of two-level configuration mixing in the $\underline{|1, 0^-\rangle}$ and $\underline{|2, 0^-\rangle}$ states at $E_x = 5280, 5599$ keV. Residual interaction $\mathbf{v}$ is decomposed into m.e. v_{11} and v_{22} describing the shift of the two levels and m.e. $v_{12} = v_{21}$ describing the level repulsion.

be described as

$$\underline{|n, 1^-\rangle} = t_{n1}(1^-)\,|s_{1/2}p_{1/2}, 1^-\rangle + t_{n5}(1^-)\,|d_{3/2}p_{1/2}, 1^-\rangle + \sum_{q=2-4,6-9} t_{nq}(1^-)\,|C_q, 1^-\rangle. \quad (11)$$

For the 1^- states, a deviation matrix similar to Eqs. (9) and (10) can be defined with elements $d_{n1}(1^-)$, $d_{n5}(1^-)$, referring to the two configurations excited by ^{207}Pb(d, p), namely, $s_{1/2}p_{1/2}$ and $d_{3/2}p_{1/2}$.

E. Excitation energies

Up to the lowest proton particle-hole configuration, using the energies of the known single-particle and single-hole states in the lead region [8], the lowest 1p-1h configurations in ^{208}Pb with spin 0^- are predicted as

Configuration		Energy (keV)	
$\|6, 0^-\rangle$	...	...	
$\|5, 0^-\rangle$	$\pi p_{3/2}d_{3/2}$	$e_5^0(0^-) = 7383,$	$(7383 = 7683 - 300^{a})$
$\|4, 0^-\rangle$	$\nu\, d_{3/2}p_{3/2}$	$e_4^0(0^-) = 6866,$	
$\|3, 0^-\rangle$	$\nu\, g_{9/2}h_{9/2}$	$e_3^0(0^-) = 6844,$	
$\|2, 0^-\rangle$	$\nu\, d_{5/2}f_{5/2}$	$e_2^0(0^-) = 5568,$	
$\|1, 0^-\rangle$	$\nu\, s_{1/2}p_{1/2}$	$e_1^0(0^-) = 5463.$	(12)

The gap Δ between the second and third configuration, $|2, 0^-\rangle$ and $|3, 0^-\rangle$, is 1276 keV, see Fig. 1. It is more than ten times larger than the m.e. of the residual interaction of about 100 keV according to Refs. [4,5]. Hence the mixing between the two lowest 0^- configurations in ^{208}Pb represents an excellent example of a two-level scheme.

[a]The Coulomb shift is assumed to be 300 keV [5].

The excitation energies of the two states are obtained from Table I,

$$E_1(0^-) = 5280\,\text{keV}, \quad E_2(0^-) = 5599\,\text{keV}. \quad (13)$$

III. EXPERIMENTAL DATA

A. Experiments with Q3D magnetic spectrograph

Using the Q3D magnetic spectrograph of the tandem accelerator of the Maier-Leibnitz laboratory at München, experiments of the reactions ^{207}Pb(d, p) and ^{208}Pb(p, p') via isobaric analog resonances in ^{209}Bi (IAR-pp') were performed. They are described in detail in Ref. [6]. The resolution of about 3 keV, the low background (up to 1:5000), a reliable identification of contamination lines from light nuclei, and a sophisticated fit of the spectra by the computer code GASPAN [10], allow us to resolve nearby levels and to detect weakly excited states even as neighbors to hundred times stronger levels. Here we refer to data obtained from the ^{207}Pb(d, p) experiment in the region $E_x = 5.2$–5.7 MeV. Compared with earlier work with a resolution of 18 keV using the Heidelberg multigap magnetic spectrograph [11] and following work in Refs. [3,8,12,13], the resolution has been improved and the background lowered.

The mean level spacing is about 6 keV in the regions near the two 0^- states. Peaks are identified by comparison with the known data [3,12–16], see Table I. A comparison to the preliminary analysis of the ^{208}Pb(p, p') data on seven IAR in ^{209}Bi with similar resolution [6] allows us to verify the identifications.

Figures 2 and 3 show two 0.1 MeV long extracts of ^{207}Pb(d, p) spectra, each covering 1.2 MeV totally. Whereas the neighbors of the 5599 0^- state are 12–15 keV away, the 5280 0^- state is surrounded by two levels at a 4–7 keV distance. At scattering angles of $\Theta = 20°$–$30°$, the 5276 and 5287 states are excited with cross sections of 1–20% of the 5280 state.

Peaks from light contaminations (^{12}C, ^{14}N, ^{16}O, ^{23}Na, and more) are identified in the whole spectra by the kinematic shift in a series of spectra taken at scattering angles $\Theta = 20°$–$30°$ and the kinematic broadening for different openings of the entrance slit to the Q3D magnetic spectrograph, see Ref. [6]. In the region of $E_x = 5.5$–5.7 MeV, contamination lines from ^{14}N with cross sections of a few μb/sr are detected at scattering angles $\Theta = 20°$ and $30°$.

TABLE I. Levels near the 5280 0^- and 5599 0^- states in ^{208}Pb (marked •). Within 1–2 keV, the energy label corresponds to the energies from Refs. [3,13–16] or this work. The values from Refs. [13] refer to the reaction ^{208}Pb(p, p') at $E_p = 22$ MeV. Spin and parity I^π from Refs. [3,6,15,16] are shown. Using the technique [17] to decompose a line in a γ-ray spectrum into a sum and a direct part, the excitation energies from Ref. [14] are updated in Ref. [15]; in effect, they have changed by about 0.3 keV, more than the given experimental error. For 1^- states, the corrected excitation energies are generally up to 1 keV lower than those given in Ref. [14], but for other spins they tend to be higher.

	Energy label	E_x (keV)				I^π	Ref.
		This work	Ref. [3]	Ref. [15]	Ref. [13]		
				Region near 5280 0^- and 5292 1^-			
	5239	5239.5±0.8	5239.35±0.36			4^-	[6]
	5241		5241.0±0.4[a]		5240.8±1.5	0^+	[16]
	5245	5245.4±0.3	5245.28±0.06	5245.2±0.1	5244.6±1.0	3^-	[3]
	5254	5254.2±0.8	5254.16±0.15				
	5261	5261.2±0.8					
	5266	5266.6±0.9					
	5276	5276.3±0.4			5277.1±1.5	4^-	[6]
•	5280	5280.5±0.1	5280.32±0.08	5280.5±0.1	5281.3±1.5	0^-	[3]
	5287	5287.8±1.9			5287.2±1.5		
	5292	5292.2±0.1	5292.00±0.20	5292.1±0.1	5292.6±1.5	1^-	[3]
	5307	5307.6±1.5					
	5316	5313.0±1.0	5317.00±0.22			(3^+)	[3]
	5317	5316.9±1.5	5317.30±0.60		5317.7±0.6		
	5326				5326.9±0.6		
	5339	5340.0±0.9	5339.46±0.16		5340.1±1.5	8^+	[3]
	5347	5347.4±0.2	5347.15±0.25		5348.4±0.6	3^-	[3]
				Region near 5599 0^-			
	5548	5548.5±0.4	5548.08±0.20	5548.2±0.1	5547.5±1.5	2^-	[3]
	5557	5557.2±1.0			5554.0±2.0		
	5563	5563.9±0.3	5563.58±0.14	5563.6±0.1	5564.7±0.6	$3^-, 4^-$	[3]
	5566		5566.00±0.60			4^-	[3]
	5572	5572.0±0.8					
	5577	5579.0±0.9			5576.6±1.5		
	5587	5587.4±1.0			5587.7±0.5		
•	5599	5599.8±0.5	5599.40±0.08	5601.7±0.1	5599.6±0.4	0^-	[3]
	5614	5614.4±1.7			5615.4±0.4		
	5641	5640.7±0.6	5641.10±0.50	5641.4±0.5	5639.9±1.5	$(1^-, 2^+)$	[14,15]
	5643				5643.1±1.5		
	5649	5648.7±0.5	5649.70±0.28		5649.8±0.9	(5^-)	[3]

[a]From Ref. [16].

B. Extraction of relative spectroscopic factors

By use of the GASPAN code [10] with the option of fixed energy distances, and the excitation energies from Table I, the cross sections are precisely determined. Figures 2 and 3 show spectra for the regions around the 5280 0^- and the 5599 0^- levels. Table II shows the cross sections for the 5280 0^-, 5292 1^- and 5599 0^- levels. They increase by a factor of 4 between $\Theta = 20^\circ$ and30°. In relation to the 5292 1^- state, the cross sections for the two 0^- states differ by a constant factor (0.32 and 0.05) within the errors. For $\Theta = 20^\circ$–30°, distorted-wave Born approximation (DWBA) calculations [12,13] yield the steep slope observed for $L = 0$ [12,13]. In contrast, the angular distributions for the two levels 5924 2^-, 5947 1^- [3], bearing the main strength of the $d_{3/2}p_{1/2}$ configuration, vary by less than 10% for $\Theta = 20^\circ$–30°.

TABLE II. For the two 0^- states at $E_x = 5280, 5599$ MeV and the 5292 1^- state, the mean cross section from six runs taken with different slit openings of the Q3D spectrograph [6] and evaluated with different methods of background subtraction [10]. The angular distributions for the 5292 1^-, 5280 0^-, 5599 0^- states have similar slopes in congruence with DWBA calculations [12,13]. They scale as 1 : 0.32 : 0.05, respectively, and rise from $\Theta = 20^\circ$ to 30° by a factor of 4.

Energy label	Spin	$d\sigma/d\Omega(\mu$b/sr)		
		$\Theta = 20^\circ$	$\Theta = 25^\circ$	$\Theta = 30^\circ$
5280	0^-	90.8±5.6	2546±8.0	361.8±15.2
5292	1^-	291.8±15.4	7887±19.5	1131.1±36.0
5599	0^-	11.4±2.3	424±1.6	58.2±2.2

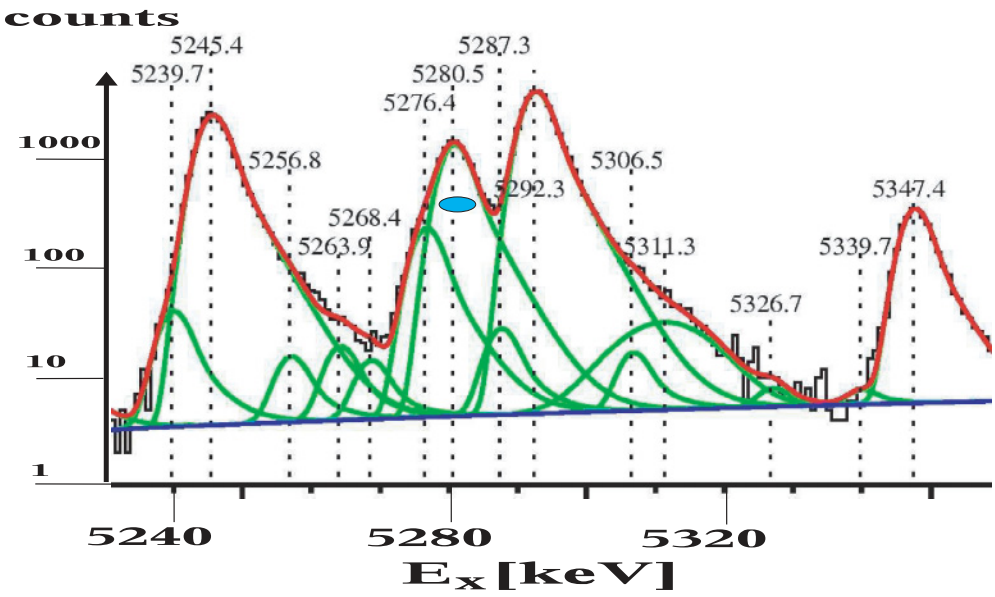

FIG. 2. (Color online) ^{207}Pb(d, p) spectrum taken at $\Theta = 30^\circ$ for $E_x = 5.23$–5.36 MeV. The 5280 0^- state (marked •) is resolved from the two neighbors in 4–7 keV distance. It is displayed on a logarithmic scale because the background is 1/2000 of the maximum peak, but many levels with 1% of the maximum are clearly resolved. Curves show the fit by the computer code GASPAN [10], where the energies are taken from Table I and only the centroid of all energies together and the peak heights are varied. The widths and tails are interpolated from a table generated by inspection of several strong, rather isolated peaks in the whole spectrum covering about 1.2 MeV, nearly ten times more than shown. A weak contamination line from ^{23}Na is identified near $E_x = 5.31$ MeV.

In view of the steep rise of the angular distribution from $\Theta = 20^\circ$ to $\Theta = 30^\circ$, we determine relative spectroscopic factors by first calculating a mean angular distribution of the three states,

$$\widetilde{R}(\Theta) = \sum_{n,I^\pi} \left\{ \frac{d\sigma}{d\Omega}(|n, I^\pi\rangle, \Theta) \Big/ \sum_\theta \frac{d\sigma}{d\Omega}(|n, I^\pi\rangle, \Theta) \right\}. \quad (14)$$

The energy dependence of the cross section is neglected because of the small energy range. In a least squares fit, we then obtain the mean cross section for the state $|n, I^\pi\rangle$

$$\left\langle \frac{d\sigma}{d\Omega}(|n, I^\pi\rangle) \right\rangle = \sum_\theta \left\{ \frac{d\sigma}{d\Omega}(|n, I^\pi\rangle, \Theta) \Big/ \widetilde{R}(\Theta) \right\} \quad (15)$$

as a measure of the relative spectroscopic factors. In Table III we adjust the mean values to the cross section of the 5292 1^- state at the scattering angle $\Theta = 25^\circ$.

C. Determination of mixing amplitudes

The unitarity relation for a two-level space [Eq. (9)] and the assumption of a vanishing deviation matrix $d_{kl}(0^-)$ [Eq. (10)] yields only one independent variable, since $t_{11}^2 + t_{21}^2 = 1$ and $t_{22}^2 + t_{12}^2 = 1$. The reaction ^{207}Pb(d, p) excites solely the $s_{1/2}p_{1/2}$ component of the 0^- states [Eq. (7)]. Thus, the ratio of the measured mean cross sections (Table III) is

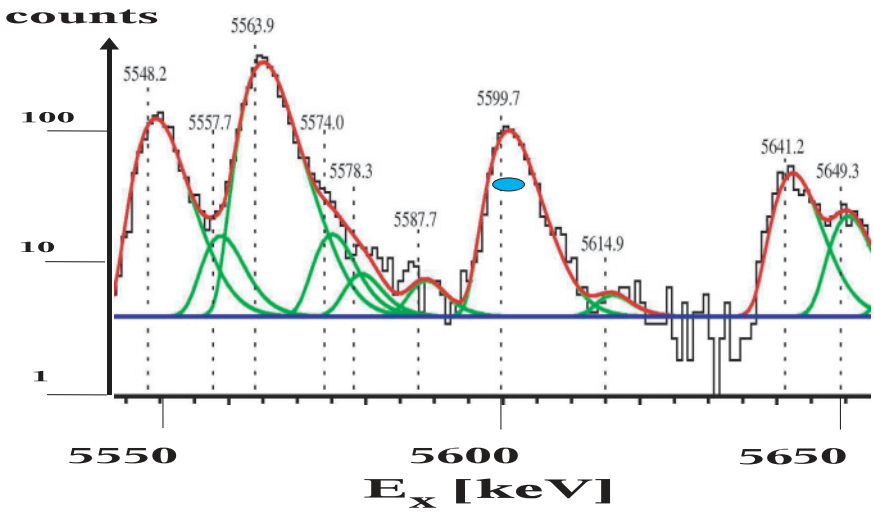

FIG. 3. (Color online) ^{207}Pb(d, p) spectrum taken at $\Theta = 25^\circ$ for $E_x = 5.54$–5.65 MeV. The 5599 0^- state (marked •) is well isolated. For other details, see Fig. 2.

TABLE III. Up to $E_x = 6.5$ MeV, two states (in bold) with spin 0^- (marked •) and nine states with spin 1^- are known. Within 1–2 keV, the energy label reflects the energies E_x from Refs. [3,12–15] or this work. Their mean cross section $\langle \frac{d\sigma}{d\Omega}(|\underline{n, I^\pi}\rangle)\rangle$ [see Eq. (15)] adjusted to reproduce the cross section at $\Theta = 25^\circ$ for the 5292 1^- state is shown. Spectroscopic factors $S_{(d,p\gamma)}$ [3] and S.F. [12,13] are given for comparison. The reaction ^{207}Pb(d, p) was measured with the same deuteron energy $E_d = 22.000$ MeV as in Refs. [12,13]. In the states with spin 1^-, the $L = 0$ and $L = 2$ transfer excites the $s_{1/2}p_{1/2}$ and $d_{3/2}p_{1/2}$ configurations, respectively, but in the two 0^- states only the $s_{1/2}p_{1/2}$ component is excited by the $L = 0$ transfer [Eqs. (7), (11)]. For the nine 1^- states, from the measured angular distributions, we derive the ratio $r_{n51}(1^-)$ of the strength for the configurations $d_{3/2}p_{1/2}$ ($L = 2$) and $s_{1/2}p_{1/2}$ ($L = 0$), see Eq. (18).

State	Energy label	I^π	L	$S_{(d,p\gamma)} \times 1000$ Ref. [3]	L	$S.F. \times 1000$ Refs. [12,13]	$r_{n51}(1^-)$	$\langle \frac{d\sigma}{d\Omega}(\underline{\lvert n, I^\pi\rangle})\rangle$ (μb/sr) This work
$\underline{\lvert 1, 1^-\rangle}$	4841	1^-	0	11±4			>0.5	22±5
$\underline{\lvert \mathbf{1}, \mathbf{0}^-\rangle}$	**5280**	0^-	0	377±32	0	650	•	250±10
$\underline{\lvert 2, 1^-\rangle}$	5292	1^-	0	1071±325	0	1550	<0.1	785±30
$\underline{\lvert 3, 1^-\rangle}$	5512	1^-	0	74±22			>0.8	160±15
					2	165		
$\underline{\lvert \mathbf{2}, \mathbf{0}^-\rangle}$	**5599**	0^-	0	60±6	0	103	•	40±5
$\underline{\lvert 4, 1^-\rangle}$	5641	1^-[a]		4[b]			>0.7	22±3
$\underline{\lvert 5, 1^-\rangle}$	5947	1^-	2	1266±488	2	1390	>12[c]	1300±80[d]
$\underline{\lvert 6, 1^-\rangle}$	6263	1^-	2	55±23	2	7	>0.6	25±10
					0	59		
$\underline{\lvert 7, 1^-\rangle}$	6314	1^-	2	88±38	0	113	>0.7	38±12
$\underline{\lvert 8, 1^-\rangle}$	6360	1^-	2	29±13	2	13	>0.7	9±3
$\underline{\lvert 9, 1^-\rangle}$	6486	1^-[e]		30[b]	2	38	>0.8	30±5
					0	12		

[a] $I^\pi = (1^-, 2^+)$ from Refs. [14,15]. The preliminary analysis of our IAR-pp' data excludes spin 2^+.
[b] Derived from the relative population strength ($S_{\text{exp.}}$).
[c] By comparison with the 5924 2^- state with $L = 2$ only.
[d] The error includes the variation of the angular distribution with Θ.
[e] $I^\pi = 1^-$ from Refs. [14,15].

used to derive the two-level matrix **t**,

$$t_{21}^2(0^-)/t_{11}^2(0^-) = \left\langle \frac{d\sigma}{d\Omega}(\underline{|2, 0^-\rangle}) \right\rangle \Big/ \left\langle \frac{d\sigma}{d\Omega}(\underline{|1, 0^-\rangle}) \right\rangle. \quad (16)$$

Explicitly, we have

$$\begin{aligned} |t_{11}(0^-)| &= |t_{22}(0^-)| = 0.928 \pm 0.015, \\ |t_{12}(0^-)| &= |t_{21}(0^-)| = 0.37 \pm 0.04. \end{aligned} \quad (17)$$

D. Completeness in the truncated configuration space

An essential assumption is the proportionality of the sum of the $s_{1/2}p_{1/2}$ strength in all states for spins $I^\pi = 0^-, 1^-$ to the spin factor $(2I + 1)$. Yet the 1^- states contain also the configuration $d_{3/2}p_{1/2}$ which is excited by ^{207}Pb(d, p), too. In the following, we disentangle these two components excited by $L = 0$ and $L = 2$ transfer.

Higher 0^- states are not known, but they should have energies above $E_x \approx 6.8$ MeV, see Fig. 1. In contrast, up to $E_x = 6.5$ MeV, nine 1^- states are known as predicted by the shell model.

The cross sections $\langle \frac{d\sigma}{d\Omega}(|\underline{n, I^\pi}\rangle)\rangle$ for the two 0^- states and all 1^- states up to $E_x = 6.5$ MeV (Table III) are consistent with the data of Refs. [12,13] within the errors. The ratios agree also with the population strengths of Ref. [3], but they are more precise.

The reaction ^{207}Pb(d, p) excites the two configurations $s_{1/2}p_{1/2}$ and $d_{3/2}p_{1/2}$ in all 1^- states but only the configuration $s_{1/2}p_{1/2}$ in the 0^- states. The sum of the $s_{1/2}\,p_{1/2}$ strength in the two 0^- states is derived from Refs. [3] and [12,13] as 80% and 130%, respectively, see Table III. As noted by Ref. [12], the DWBA calculations for $L = 0$ are extremely sensitive to the shape of the potential.

We assume the two 0^- states to contain the $s_{1/2}\,p_{1/2}$ strength almost completely. Because higher configurations admix little due to the gap Δ between the second and third 0^- configurations, $d_{5/2}f_{5/2}$ and $g_{9/2}h_{9/2}$, being larger than ten times the mean m.e. of the residual interaction (about 100 keV), the deviation matrix $d_{kl}(0^-)$ is expected to almost vanish [Eq. (10)]. By comparing the detected strength of the $s_{1/2}p_{1/2}$ 0^- and $s_{1/2}p_{1/2}$ 1^- configurations, we try to minimize the deviation matrices $d_{n1}(1^-)$, $d_{n5}(1^-)$. In effect, upper limits of the deviation matrix element $d_{11}(0^-) \approx d_{22}(0^-)$ and an estimate of the missing strength $\sum_{n\geqslant 2} t_{n1}^2(0^-)$ are derived.

The 5292 1^- state contains less than 93% of the $s_{1/2}p_{1/2}$ strength, since the ratio of its cross section to the sum of the two 0^- states is less than the ratio 3:1 expected from the spin factor

$(2I+1)$, see Table II. Other 1^- states contain the remaining $s_{1/2}p_{1/2}$ strength, but the 5292 1^- state contains also some of the $d_{3/2}p_{1/2}$ strength [besides other configurations not detected by ^{207}Pb(d, p) but by IAR-pp']. The missing $s_{1/2}p_{1/2}$ strength is contained in the other eight 1^- states.

Whereas the angular distribution for $L=0$ between $\Theta = 20^\circ$ and 30° changes by a factor of 4, the angular distribution for $L=2$ is rather flat [12,13]. We determine for each 1^- state a ratio

$$r_{n51}(1^-) = t^2_{n5}(1^-)/t^2_{n1}(1^-), \tag{18}$$

where the amplitudes $t_{n1}(1^-)$, $t_{n5}(1^-)$ are defined in Eq. (11). Only upper or lower limits can be given (Table III) since the configurations $s_{1/2}p_{1/2}$ and $d_{3/2}p_{1/2}$ are concentrated in the 5292 1^- and 5947 1^- states, respectively, and all other 1^- states are weakly excited by ^{207}Pb(d, p).

(i) All 1^- states except for the 5292 1^- state listed in Table III have rather flat angular distributions for $\Theta = 20^\circ$–30°. For the states considered, the dependence of the cross section on the energy E_x for states with the same configuration mixture is negligible [12,13].

(ii) For the 5924 2^- and 5947 1^- states, the angular distribution for $\Theta = 20^\circ$–30° is flat (similar to that for other states with dominant $d_{5/2}p_{1/2}$ strength) in contrast to the steep rise for the $s_{1/2}p_{1/2}$ configuration [12,13]. The 5924 2^- and 5947 1^- states contain most of the $d_{3/2}p_{1/2}$ strength [13], and the spin assignments are firm [3].

(iii) In the 5947 1^- state, the comparison of the shape of the angular distribution to the 5924 2^- state allows us to deduce an upper limit for the $s_{1/2}p_{1/2}$ strength of about 8% or a ratio $r_{n51}(1^-) > 12$ [Eq. (18)].

(iv) For the other 1^- states besides the 5292 and 5947 states, lower limits of the ratio $r_{n51}(1^-)$ are derived, see Table III.

(v) The deviation of the slope of the cross section for the 5292 1^- state compared with that for the two 0^- states, especially at $\Theta = 20^\circ$, implies up to 10% $d_{3/2}p_{1/2}$ admixture (Table II).

Summing the thus derived upper limits of $s_{1/2}p_{1/2}$ admixtures $t^2_{n1}(1^-)$ to all other 1^- states, we derive a lower limit 86% of the $s_{1/2}p_{1/2}$ configuration in the 5292 1^- state and the $d_{3/2}p_{1/2}$ strength in the 5947 1^- state to be $80\% \pm 5\%$. Together with the upper limit of 93% derived before, the sum of the $s_{1/2}p_{1/2}$ strength in all nine 1^- states is found to be complete within a margin of 8%.

We conclude that the sum of the $s_{1/2}p_{1/2}$ strength in the 5280 0^- and 5599 0^- states is complete within better than 97% or $d_{11}(0^-) \approx d_{22}(0^-) < 0.03$. The elements $d_{12}(0^-) \approx d_{21}(0^-)$ are obtained by considering in addition the experimental errors of the amplitudes $t_{nk}(0^-)$. An upper limit for the deviation matrix [Eq. (10)] is thus obtained,

$$\begin{aligned} d_{11}(0^-) &\approx d_{22}(0^-) < 0.03, \\ |d_{21}(0^-)| &\approx |d_{12}(0^-)| < 0.02. \end{aligned} \tag{19}$$

IV. RESULTS AND DISCUSSION

A. Determination of matrix elements of the residual interaction from ^{207}Pb(d, p)

Using Eq. (8), we derive the m.e. of the residual interaction for the two-level space consisting of the configurations $|s_{1/2}p_{1/2}0^-\rangle$ and $|d_{5/2}f_{5/2}0^-\rangle$ from experimental data. Omitting the notation referring to spin 0^-, we have explicitly

$$\begin{aligned} v_{11} &= t^2_{11}E_1 + t^2_{21}E_2 - \left(t^2_{11} + t^2_{21}\right)e^0_1, \\ v_{22} &= t^2_{12}E_1 + t^2_{22}E_2 - \left(t^2_{12} + t^2_{22}\right)e^0_2, \\ v_{12} &= t_{11}t_{12}E_1 + t_{21}t_{22}E_2 \\ &\quad - \tfrac{1}{2}(t_{11}t_{12} + t_{21}t_{22})\left(e^0_1 + e^0_2\right), \\ v_{21} &= t_{12}t_{11}E_1 + t_{22}t_{21}E_2 \\ &\quad - \tfrac{1}{2}(t_{12}t_{11} + t_{22}t_{21})\left(e^0_1 + e^0_2\right). \end{aligned} \tag{20}$$

Here, the shell model energies e^0_k are given in Eq. (12), the energies E_n of the two states in Eq. (13). From the experimental data, the amplitudes $\mathbf{t}$ of the two states are derived in Eq. (17). We obtain the m.e.

$$\begin{aligned} v_{11} &= -140 \pm 10\,(\text{exp.}) \pm 20\,(\text{syst.})\ \text{keV}, \\ v_{22} &= -10 \pm 10\,(\text{exp.}) \pm 20\,(\text{syst.})\ \text{keV}, \\ |v_{12}| &= |v_{21}| = 110 \pm 10\,(\text{exp.}) \pm 15\,(\text{syst.})\ \text{keV}. \end{aligned} \tag{21}$$

The sign of the off-diagonal terms $v_{12} = v_{21}$ cannot be determined from our data. The diagonal terms v_{11}, v_{22} describe the level shift, the off-diagonal terms $v_{12} = v_{21}$ the level repulsion, see Fig. 1.

The m.e. of the residual interaction (especially the off-diagonal m.e.) agree with the mean m.e. of about 100 keV obtained from the analysis of the lowest 20 particle-hole configurations in ^{208}Pb [4,5]. The values $\mathbf{v}$ are compatible with theoretical calculations [1,2], but they are more precise.

The systematic error as given by the uncertainty of the value $r_{kl}(I^\pi)$ in Eq. (8) is estimated from the extension of the two-level scheme into a three-level scheme. By adding a fictitious configuration at $e^0_3 = e^0_2 + \Delta$ (see Fig. 1) with a fixed strength $t^2_{33} = 1 - d_{11}$ [see Eq. (19)] and optimizing the unitarity of the 3×3 matrix t_{kn} by varying only the amplitudes t_{13}, t_{23} and t_{31}, t_{32} within the uncertainties, estimates of 20 and 15 keV for the systematic errors of the diagonal and off-diagonal m.e., respectively, are obtained. These values can be trusted since all m.e. involved with the fictitious configuration are less than the mean m.e. of about 100 keV [4,5].

B. Data from IAR-pp'

A preliminary analysis of the IAR-pp' data [6] is consistent with the spin assignments given in Table III. Especially the 5292 1^-, 5924 2^-, 5947 1^- states are selectively excited by the $s_{1/2}$, $d_{3/2}$, and $d_{3/2}$ IAR, respectively.

In early IAR-pp' experiments [7], excitation functions were measured for several multiplets with a resolution of 26 keV. The energies given by Ref. [7] derive from the calibration of IAR-pp' spectra taken with the Enge split-pole magnetic spectrograph [18]. They are about 0.13% too low [6].

Measurements of the excitation function for the unresolved 5280 0^-, 5292 1^- doublet (5.284 MeV) show a strong excitation by the $s_{1/2}$ IAR. A weak excitation by the $d_{5/2}$ IAR is explained by the $d_{5/2}f_{5/2}$ component in the 5280 0^- state [Eqs. (7), (17)] and $d_{5/2}f_{5/2}$, $d_{5/2}p_{3/2}$ components in the 5292 1^- state [Eq. (11)].

Similarly, the resolved 5924 2^-, 5947 1^- doublet (5.914 + 5.936 MeV) is dominantly excited by the $d_{3/2}$ IAR, proving the presence of about equal $d_{3/2}p_{1/2}$ components in both states in agreement with the results from ^{207}Pb(d, p). Whereas the 5924 2^- state clearly resonates on the $s_{1/2}$ IAR (which is explained by weak $s_{1/2}f_{5/2}$ and $s_{1/2}p_{3/2}$ components), the decay curve of the 5947 1^- state near the $s_{1/2}$ IAR is smooth in congruence with the value $r_{n51}(1^-)$ given in Table III for $n = 5$.

The $d_{5/2}$ and $s_{1/2}$ IAR are overlapping, $E^{\mathrm{res}} =$ 16.496, 16.965 MeV and $\Gamma^{\mathrm{tot}} = 308, 319$ keV, respectively [6,7]. Neglecting the interference and using the amplitudes of Eq. (17), a calculation of the cross sections for the 5280 0^- and 5599 0^- states on the $d_{5/2}$ and $s_{1/2}$ IAR (using the IAR parameters of Ref. [6]) roughly agrees with the measured data. An attempt following Ref. [19] to describe the angular distributions by interfering IAR did not yield conclusive results, essentially because of missing data at scattering angles $\Theta < 40^\circ$.

V. SUMMARY

Up to $E_x = 6.1$ MeV, the shell model predicts 120 one-particle one-hole states in ^{208}Pb (70 states with negative and 50 states with positive parity). However, only two states with spin 0^- are known. From a measurement of the reaction ^{207}Pb(d, p) with an energy resolution of 3 keV, we identify the two known states with spin 0^- among about 150 physical states. The mean level spacing in the region of $E_x = 5.2$–5.7 MeV around the two 0^- states is 6 keV. Spectroscopic information from ^{207}Pb(d, p) is used to determine their structure. Data from inelastic proton scattering via IAR in ^{209}Bi support the structure information.

Among all levels in doubly magic nuclei [8,9], few states with spin 0^- are known, all of them are unbound except for two states in ^{208}Pb. The 0^- doublet in ^{208}Pb represents a rare case of a close pair of 0^- states with a large distance to the next 0^- configuration predicted by the shell model. So, this doublet represents a unique case of a two-level mixing.

Matrix elements of the residual interaction between the two lowest 0^- configurations in ^{208}Pb are derived from the experimental data. Spectroscopic information from the nine lowest 1^- states is used to quantify the systematic uncertainty. The value of the off-diagonal mixing strength is determined as $110 \pm 10\,(\mathrm{exp.}) \pm 15\,(\mathrm{syst.})$ keV, but the sign is not determined. The precision is higher than that attained with current shell model calculations.

ACKNOWLEDGMENTS

This work has been supported by MLL, DFG C4-Gr894/2-3, and DFG Br799/12-1.

[1] B. A. Brown, Phys. Rev. Lett. **85**, 5300 (2000).
[2] M. Rejmund, M. Schramm, and K. H. Maier, Phys. Rev. C **59**, 2520 (1999).
[3] M. Schramm, K. H. Maier, M. Rejmund, L. D. Wood, N. Roy, A. Kuhnert, A. Aprahamian, J. Becker, M. Brinkman, D. J. Decman, E. A. Henry, R. Hoff, D. Manatt, L. G. Mann, R. A. Meyer, W. Stoeffl, G. L. Struble, and T.-F. Wang, Phys. Rev. C **56**, 1320 (1997).
[4] A. Heusler and P. von Brentano, Ann. Phys. (NY) **75**, 381 (1973).
[5] A. Heusler, G. Graw, R. Hertenberger, F. Riess, H.-F. Wirth, T. Faestermann, R. Krücken, J. Jolie, N. Pietralla, and P. von Brentano, http://arXiv.org/abs/nucl-ex/0601016; A. Heusler, http://www.mpi-hd.mpg.de/personalhomes/hsl.
[6] A. Heusler, G. Graw, R. Hertenberger, F. Riess, H.-F. Wirth, T. Faestermann, R. Krücken, J. Jolie, D. Mücher, N. Pietralla, and P. von Brentano, Phys. Rev. C **74**, 034303 (2006).
[7] W. R. Wharton, P. von Brentano, W. K. Dawson, and P. Richard, Phys. Rev. **176**, 1424 (1968).
[8] M. J. Martin, Nucl. Data Sheets **47**, 797 (1986).
[9] National Nuclear Data Center, Brookhaven, Evaluated Nuclear Structure Data File, http://ie.lbl.gov/ensdf/.
[10] F. Riess, http://www.cip.physik.uni-muenchen.de/~riess/.
[11] P. B. Vold, J. O. Andreassen, J. R. Lien, A. Graue, E. R. Cosman, W. Dünnweber, D. Schmitt, and F. Nusslin, Nucl. Phys. **A215**, 61 (1973).
[12] B. D. Valnion, Ph.D. thesis, Universität München, (1998), Herbert Utz Verlag, München.
[13] B. D. Valnion, V. Yu. Ponomarev, Y. Eisermann, A. Gollwitzer, R. Hertenberger, A. Metz, P. Schiemenz, and G. Graw, Phys. Rev. C **63**, 024318 (2001).
[14] E. Radermacher, M. Wilhelm, S. Albers, J. Eberth, N. Nicolay, H.-G. Thomas, H. Tiesler, P. von Brentano, and R. Schwengner, S. Skoda, G. Winter, and K. H. Maier, Nucl. Phys. **A597**, 408 (1996).
[15] E. Radermacher, M. Wilhelm, P. von Brentano, and R. V. Jolos, Nucl. Phys. **A620**, 151 (1997).
[16] M. Yeh, P. E. Garrett, C. A. McGrath, S. W. Yates, and T. Belgya, Phys. Rev. Lett. **76**, 1208 (1996).
[17] E. Radermacher, M. Wilhelm, and P. von Brentano, Nucl. Instrum. Methods **383**, 480 (1996).
[18] C. F. Moore, J. G. Kulleck, P. von Brentano, and F. Rickey, Phys. Rev. **164**, 1559 (1967).
[19] A. Heusler, M. Endriss, C. F. Moore, E. Grosse, and P. von Brentano, Z. Phys. **227**, 55 (1969).